Physical Modeling of Agitation in Refining Ladle With Submerged Lance Gas Blowing Injection: A Comparison Between Two-Nozzle and Single-Nozzle






To improve mixing phenomena during steel refining process in a ladle, it is crucial to study metal-slag interaction. Using an acrylic model, scaled 1:8, two different lances were employed: one with two nozzles (inverted T shape), and the other with a single nozzle (L shape). The effect of gas flowrate and lance position on the mixing time, dye dispersion, and the slag eye opening at the reactor surface were evaluated. Mixing time decreased and the slag eye opening area increased as the gas flow was increased from 5 L/minute to 20 L/minute. The two-nozzle lance in the radial position (2R/3) provided better results.

Authors

Davi Rodrigues de Oliveira Santos (top left), Undergraduate Student, Department of Metallurgical Engineering, Universidade Federal de Ouro Preto, Ouro Preto, MG, Brazil
davi.ros@aluno.ufop.edu.br

José Dimas de Arruda (top right), Metallurgical Engineer, Department of Metallurgical Engineering, Universidade Federal de Ouro Preto, Ouro Preto, MG, Brazil

Ana Flávia Xavier Tomás (center left), Undergraduate Student, Department of Metallurgical Engineering, Universidade Federal de Ouro Preto, Ouro Preto, MG, Brazil

Thalys Bruno de Souza Ventura (center right), Metallurgical Engineer, Department of Metallurgical Engineering, Universidade Federal de Ouro Preto Ouro Preto, MG, Brazil

Carlos Antônio da Silva (bottom left), Metallurgical Engineer, Department of Metallurgical Engineering, Universidade Federal de Ouro Preto, Ouro Preto, MG, Brazil

Johne Jesus Mol Peixoto (bottom right), Metallurgical Engineer, Department of Metallurgical Engineering, Universidade Federal de Ouro Preto, Ouro Preto, MG, Brazil

Introduction

The steel industry demands low sulfur levels in steels due to its negative effects on the alloy. For common steels, sulfur content must be below 0.015%, while for special steels, it ranges between 0.001% and 0.003%.[1] Although sulfur is removed during steelmaking and hot metal pretreatment, achieving levels below 0.01% requires additional desulfurization in secondary refining.[2] This process is carried out in the ladle furnace, where argon injection through a porous plug or submerged lance promotes the homogenization of chemical composition and temperature, in addition to assisting in the removal of inclusions and intensifying refining reactions.[3] The interaction between liquid steel, slag, gas and other elements significantly influences the behavior of inclusions.[4]

Desulfurization occurs in three zones within the reactor: the transient contact zone, where the desulfurizing agent rises to the reactor's top; the permanent contact zone, where there is continuous interaction between the slag and the metal due to the constant presence of top slag; and the rupture zone, where gas bubbles pass through the slag and escape into the atmosphere, potentially dragging liquid metal and causing reoxidation and nitrogen absorption.[5] Factors such as steel and slag composition, slag thickness and stirring rate directly influence desulfurization efficiency.[6] Studies indicate that increased bath agitation and decentralized lance positions contribute to process success.[7,8] Moreover, the lance immersion depth is crucial, as deeper immersion results in lower final sulfur content.[8,9]

The mixing of liquid steel occurs through convection and turbulent diffusion, with larger intensity at higher gas flowrates, reducing mixing time.[5,10] However, top slag can reduce process efficiency by dissipating part of the stirring energy, increasing the time required for homogenization, according to Zhou et al.[11] To improve mixing efficiency and inclusion removal, it is necessary to reduce the slag eye area, which can be achieved by reducing the gas injection hole diameter, minimizing slag entrapment and energy consumption.[12]

Gas flowrate directly affects mass transfer, promoting slag emulsification and influencing reaction rates at the slag-metal interface.[13,14] Most studies indicate that desulfurization systems require higher gas flowrates than those applied in industrial ladle furnaces.[15] However, gaps still exist in understanding plume behavior and metal-slag interaction, as well as the need for models that consolidate variables into a single equation.

Process optimization involves studying physical models on a laboratory scale to seek improvements in industrial efficiency, increasing productivity while reducing costs.[15]

This study aims to evaluate, through a physical model, the effect of gas flowrate, geometry, immersion depth, and the position of the submerged lance on mixing time, mass transfer and slag layer behavior in a ladle stirred by inert gas.

Table 1

Process Parameters and Physical Model Characteristics

Parameters	Dimensions
Maximum height of the ladle	650 mm
Liquid column height	500 mm
Diameter of the ladle	390 mm
Slag column height	20 mm
Radial distance of the submerged lance to center	0 (center); R/3; 2R/3
Distance of the submerged lance to the ladle bottom	30 mm; 50 mm and 70 mm
Gas flow	5, 7, 10, 12, 15 and 20 Nl/min.

Methodology

An acrylic model was used, built with a scaling factor of $\lambda = 1{:}8$, corresponding to an industrial reactor with an approximate capacity of 215 tons of liquid steel (Fig. 1a). For combined gas and desulfurizing material injection, the system was assembled using two models of a submerged lance: L-shaped, with a single lateral nozzle, which is directed toward the center of the ladle; and T-shaped, with two lateral injectors, separated by 180° in an inverted T-shape, with the nozzles positioned perpendicular to the ladle diameter. Three radial lance positions were evaluated, as shown in Table 1, along with other geometric data of the model.

The average mixing time was determined using the conductimetry method, with a KCl solution (15 mL) injected as a tracer at the central surface of the ladle. The salt concentration was monitored at two points: at the lateral wall, 25 cm from the bottom (CB), and at the center of the ladle bottom (CA) (Fig. 1b). Two conductivity meters recorded conductivity variations, connected to a data acquisition board integrated with software for storage and processing. The system was considered homogenized when signal variation was below 5%. Eight measurements were performed for each experimental condition, with liquid replacement after each test to prevent sensor reading saturation.

Mass transfer tests were conducted using water and soybean oil to simulate steel and slag, respectively, and thymol ($C_{10}H_{14}O$) as a sulfur tracer in steel. Experiments were carried out at 25°C, with an initial thymol concentration in water of approximately 100 ppm. For better solubilization, thymol was predissolved in analytical-grade ethanol and injected into the water via a syringe. After system homogenization, continuous oil injection through the submerged lance began, with flowrates

Figure 1

(a) Physical model of the steel ladle; (b) schematic representation of the mixing time tests; and (c) schematic representation of the mass transfer tests.

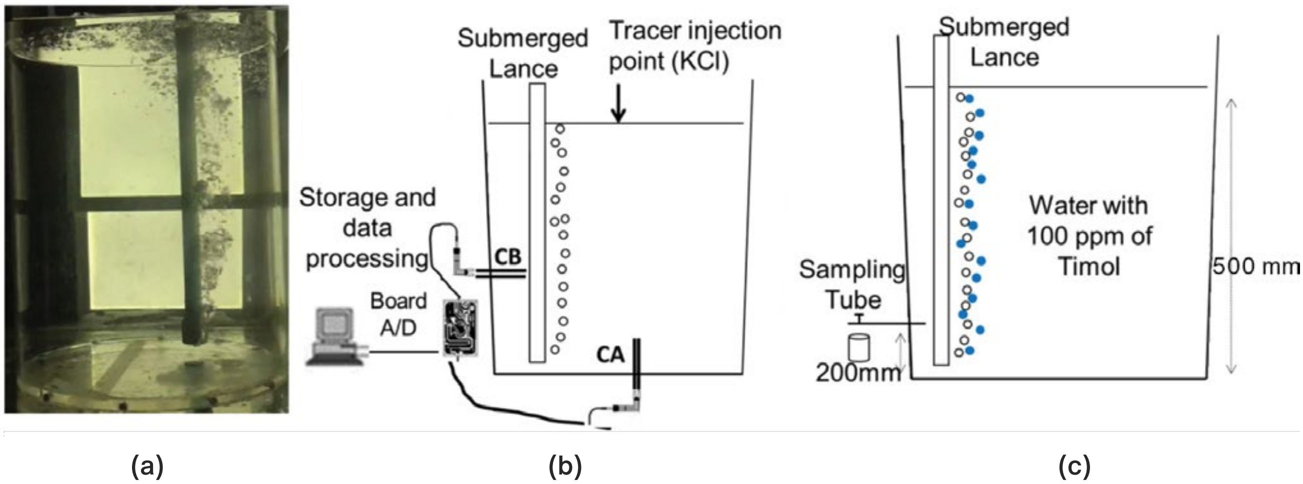

Table 2

Properties of Substances

Substance	Density (kg/m^3)	Viscosity (mPa.s)	Interfacial tension with water (mN/m)	Thymol partition coefficient
Water	998	1	—	—
Soybean oil	914.3	52.2	15.57	439.2

between 2.4 and 3.1 mL/second for 7 minutes. Every minute, 10 mL samples of aqueous solution were collected through a lateral duct 20 cm from the ladle bottom, filtered to remove oil and stored in sealed containers until analysis. Thymol concentration was determined by UV spectrophotometry (Model S100) using MetaSpec Pro software at a 275 nm wavelength, where thymol exhibits an absorption peak.

To determine the slag eye opening in the water/oil system, high-definition camera recordings were made under LED reflector illumination at the Pyrometallurgy Laboratory at the Universidade Federal de Ouro Preto's Department of Metallurgical and Materials Engineering. To facilitate oil visualization, it was dyed blue. For plume eye area calculations, images were edited with contrast enhancement, allowing for area calculation using ImageJ software. The oil-covered surface area was subtracted from the total ladle surface area to determine the slag eye opening area.

Results and Discussion

Analyzing the mixing time of a tracer injected into the physical model, it is observed that the increase in inert gas flowrate results in a reduction in mixing time under all studied conditions, similar to the study by Mazumdar et al.[16] Fig. 2a presents the average mixing time obtained in the physical model for the two conductivity meters, indicating the standard deviation for the eight measurements performed at each flowrate, considering the L-shaped submerged lance positioned at 30 mm from the bottom in three different radial positions. The results show that the most decentralized position resulted in shorter mixing times, whereas the centralized position exhibited the worst condition studied. Fig. 2b presents the mixing time results for the same submerged lance at a height of 50 mm for the radial positions R/3 and 2R/3, and at 70 mm for the centralized position. The results are similar, showing that larger decentralization leads to shorter mixing times. For the radial positions R/3 and 2R/3, variations in the height of the submerged lance with an L-shaped outlet showed minor differences (within the margin of error).

Similarly, Figs. 3a and 3b present the mixing time results for the T-shaped lance outlet. Fig. 4a shows the mixing time for three radial positions at a height of 30 mm from the bottom of the ladle. It is observed that the best condition corresponds to the most decentralized position, while the worst condition occurs at the centralized position. The same behavior is observed in Fig. 3b, which compares two decentralized positions (R/3 and 2R/3) at a height of 50 mm with the centralized position at a height of 70 mm from the bottom. Comparing the two submerged lance outlet designs, it was observed that under the same radial position and depth conditions, the T-shaped submerged lance provided better mixing conditions, achieving shorter system homogenization times. This behavior can be explained by the difference in the flow pattern formed, as the lance with more outlet holes

Figure 2

Homogenization time for L-shaped lance: At 30-mm height (a), and at 50-mm or 70-mm height (b).

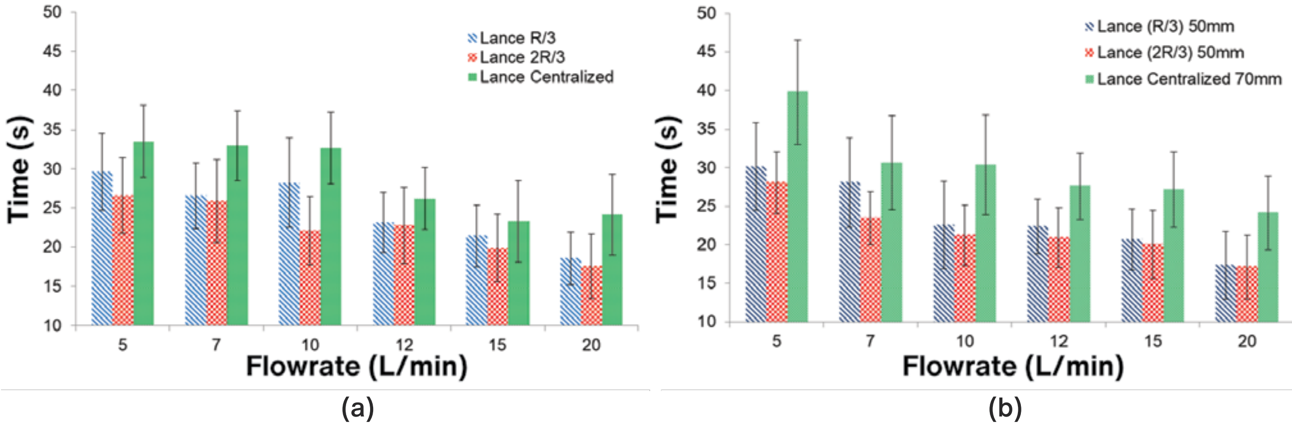

Figure 3

Homogenization time for T-shaped lance: At 30-mm height (a), and at 50-mm or 70-mm height (b).

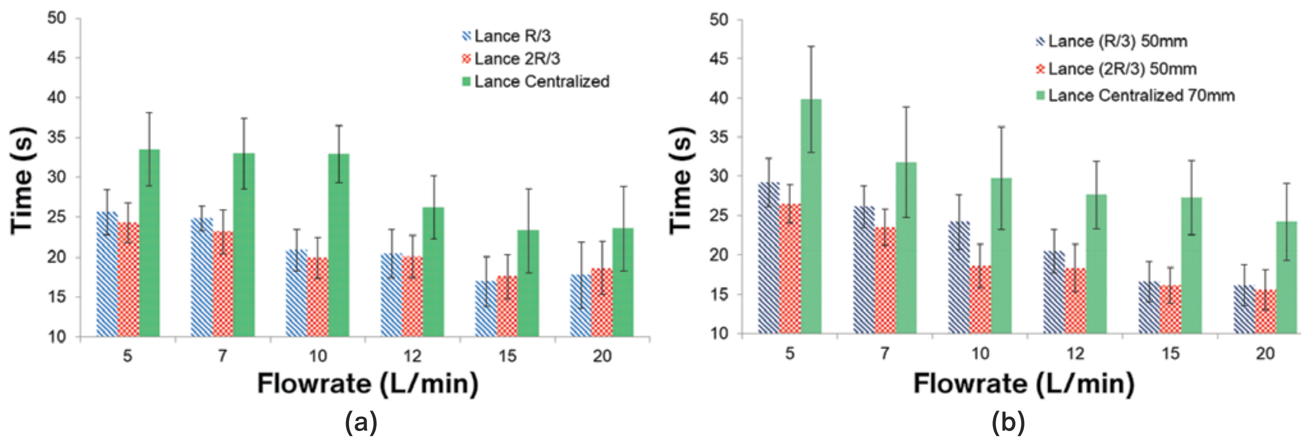

tends to provide larger bubble dispersion, which favors a shorter mixing time.[17]

The energy input (ε) for mixing was calculated as a function of the stabilization time of the tracer injected into the ladle for each studied gas flowrate. This energy input is given by Eq. 1, validated by the universal relationship shown in Eq. 2, as suggested by Szekely et al.[18] for reactors undergoing a mixing process.

$$\varepsilon = \frac{nRT}{M}\ln\left(1+\frac{\rho_{sol} g H_a}{P_a}\right)$$

(Eq. 1)

$$\tau = a \cdot \varepsilon^{-b}$$

(Eq. 2)

where

(W/kg), energy input,

(mols/second), gas flowrate,

(J/K.mol), ideal gas constant,

(K), temperature,

(kg), mass of liquid in the ladle,

(kg/m³), solution density,

(m/second²), gravitational acceleration,

(m), ladle height,

(Pa), atmospheric pressure,

(second), mixing time and

a and *b* are constants.

Figure 4

System energy as a function of mixing time for L-shaped lance: At 30-mm height (a), and 50-mm or 70-mm height (b).

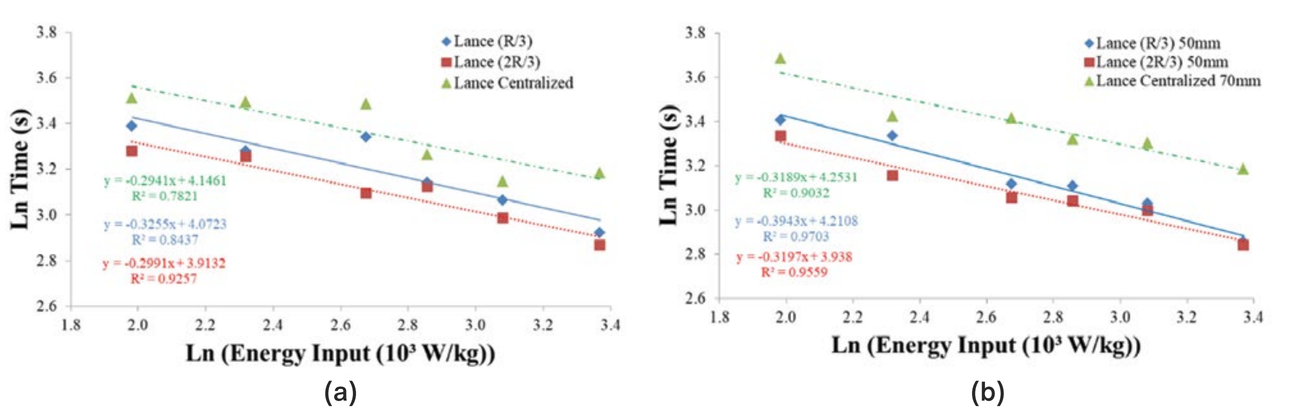

Figure 5

System energy as a function of mixing time for T-shaped lance: At 30-mm height (a) and 50-mm or 70-mm height (b).

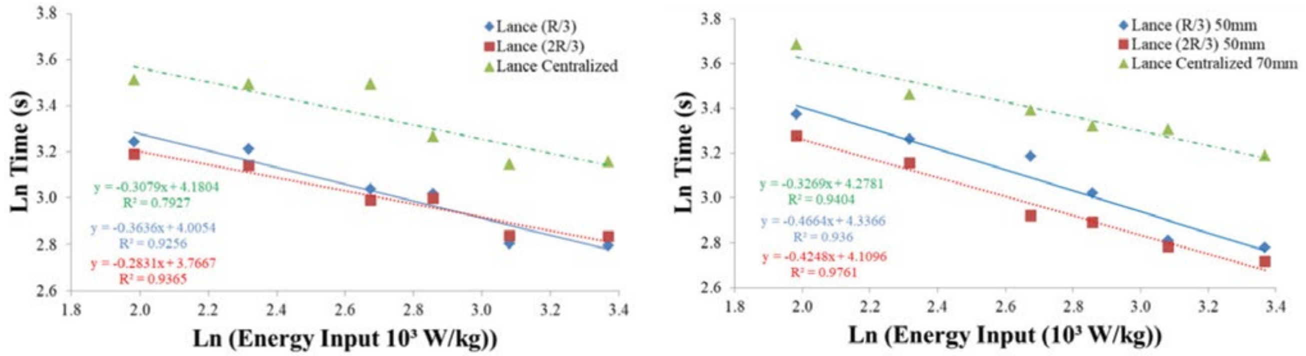

(a) (b)

Figs. 4a and 4b show the relationship between the average energy input and the mixing time recorded by the two conductivity meters, CA and CB, for the L-shaped submerged lance, considering the three radial positions and different heights relative to the bottom of the ladle. In all analyses, the stabilization time is shorter for higher energy input values, meaning that higher gas flowrates injected into the system result in shorter mixing times. Shorter mixing times at higher gas flowrates and, consequently, increased system agitation energy is consistent with the correlations found in the study by Morales et al.[12] The equations and angular coefficients indicate a steeper slope for the curves at the R/3 radial position compared to the other two positions, demonstrating a larger influence of energy input on mixing time. When comparing different immersion depths, it is observed, based on the lower values of angular coefficients, that shallower immersion depths result in a steeper curve, indicating a larger influence of energy input on mixing time.

Similarly, Figs. 5a and 5b correlate the mixing time and energy input for the T-shaped submerged lance at different radial positions and immersion depths. Higher gas injection flowrates result in shorter system mixing times. The equations and angular coefficients also indicate a steeper slope for the curves at the R/3 position, regardless of immersion depth. However, at shallower immersion depths, a larger energy input effect on mixing time is observed across all radial positions. When comparing the energy input for the T-shaped and L-shaped submerged lances (Figs. 4a and 4b), generally higher angular coefficients are observed, indicating a larger influence of energy input on mixing time for the T-shaped lance.

Mass transfer experiments were conducted by injecting oil through the submerged lance, simulating the injection of desulfurizing material into the steel. The relationship between instantaneous and initial thymol concentration (~100 ppm initial) as a function of time is given in Eq. 3,[19] which was used to obtain the curves in Fig. 6a for different gas flowrates with the L-shaped submerged lance positioned at 2R/3. A linear behavior of the curves was observed, allowing the evaluation of the behavior of K_{ap} (apparent mass transfer coefficient) as a function of time, similar to the study conducted by Silva et al.[20] Fig. 6b shows the same relationship for a gas flowrate of 10 L/minute at the three radial positions (R/3, 2R/3, and centralized). It can be observed that increasing the gas flowrate results in larger thymol extraction from water into oil. Additionally, it was observed that the radial position had little influence on the mass transfer rate.

$$\frac{C}{C_0} = e^{-K_{ap}t} \qquad \text{(Eq. 3)}$$

where

C and C_0 are the concentration at time t and the initial concentration, respectively;

K_{ap} is the apparent mass transfer coefficient.

In Figs. 7a and 7b, for the T-shaped submerged lance, it is observed that an increase in gas flowrate results in larger thymol extraction from water into oil. However, compared to the L-shaped submerged lance, lower thymol extraction was achieved under the same experimental conditions, indicating that the L-shaped lance was more efficient in the mass transfer process. For the different radial positions in Fig. 7b, the most decentralized condition showed larger efficiency in mass transfer.

Fig. 8a compares the apparent thymol extraction coefficient (K_{ap}) as a function of gas flowrate in the physical model for the two submerged lance outlet configurations, L and T: by increasing the gas flowrate, the K_{ap} value is increased. Fig. 8b compares the three radial positions

Figure 6

Linear correlation of the mass transfer rate of thymol with the submerged lance (L): Different gas flowrates in position 2R/3 (a), and 10 L/minute in different positions (b).

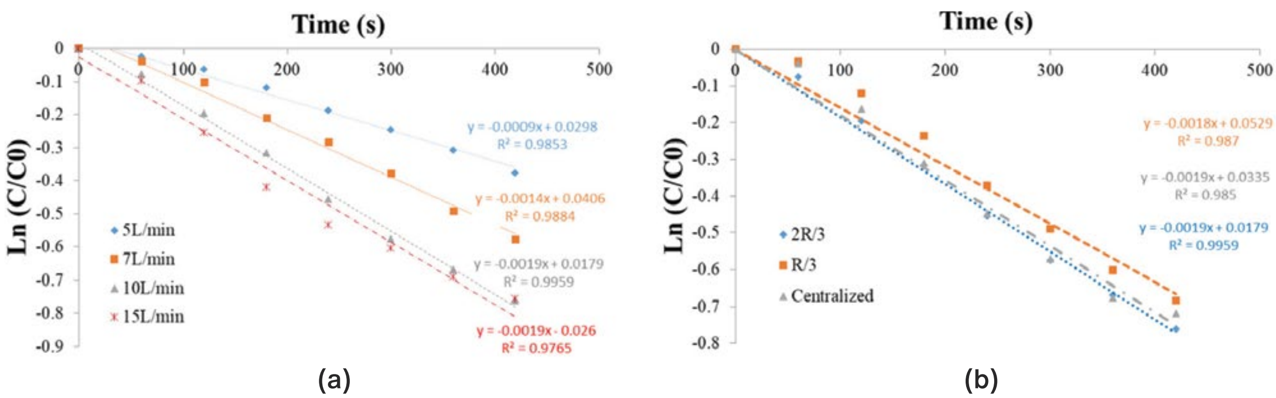

Figure 7

Linear correlation of the mass transfer rate of thymol with the submerged lance (T): Different gas flowrates in position 2R/3 (a), and 10 L/minute in different positions (b).

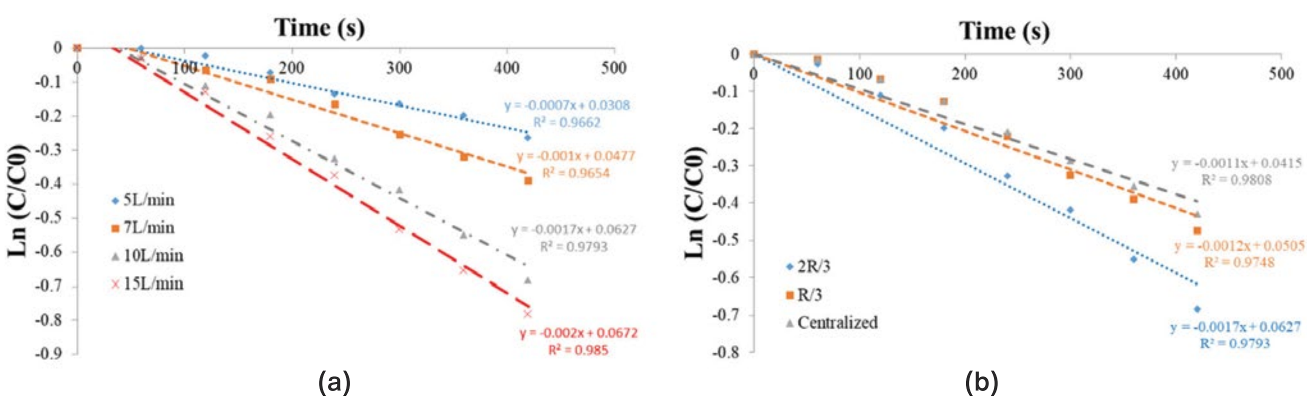

for both configurations at a gas flowrate of 10 L/minute, showing a great influence of the radial position for the T-shaped lance. It is highlighted that the value is higher for all flowrates and radial positions when using the L-shaped submerged lance. It is also noted that the best mixing time conditions were achieved with the T-shaped submerged lance, whereas the mass transfer process was favored by the L-shaped submerged lance. This can be explained by the fact that the L-shaped submerged lance has only one nozzle, providing higher gas velocity at the outlet, which can result in smaller oil droplet size and, consequently, a larger interfacial area, enhancing the mass transfer process of thymol.

The study addressed the analysis of slag eye opening and surface agitation by adding 2.4 liters of soybean oil (layer thickness ≈ 20 mm) to simulate the top slag layer on the ladle surface. Tests were conducted with both submerged lances (L and T) at three radial positions (2R/3, R/3, and Centralized) for all gas flowrates (5, 7, 10, 12, 15 and 20 L/minute). A direct relationship was observed between plume eye opening and the increase in gas flowrate. According to Morales et al.,[12] high gas flowrates and thinner slag layers reduce mixing time. Fig. 9 presents the ladle surface region for different positions at a flowrate of 10 L/minute, where visualization becomes easier due to minimal slag emulsification. For flowrates above 15 L/minute, emulsification begins to occur, showing no significant differences with further increases in flowrate but making the plume eye opening analysis more challenging. It was observed that the most decentralized position of the L-shaped submerged lance resulted in the largest plume eye opening, whereas the opposite behavior was noted for the T-shaped submerged lance, which exhibited a smaller plume eye opening at larger decentralization. This behavior can be explained by the flow direction of each submerged lance: in the L-shaped lance, the flow in more decentralized positions is directed toward the center of the ladle, while in the T-shaped configuration, the flow

Figure 8

Comparison of average K_{ap} values for the oil injection system with the submerged lance shaped in L or T: Position 2R/3 (a), and gas flow 10 L/minute (b).

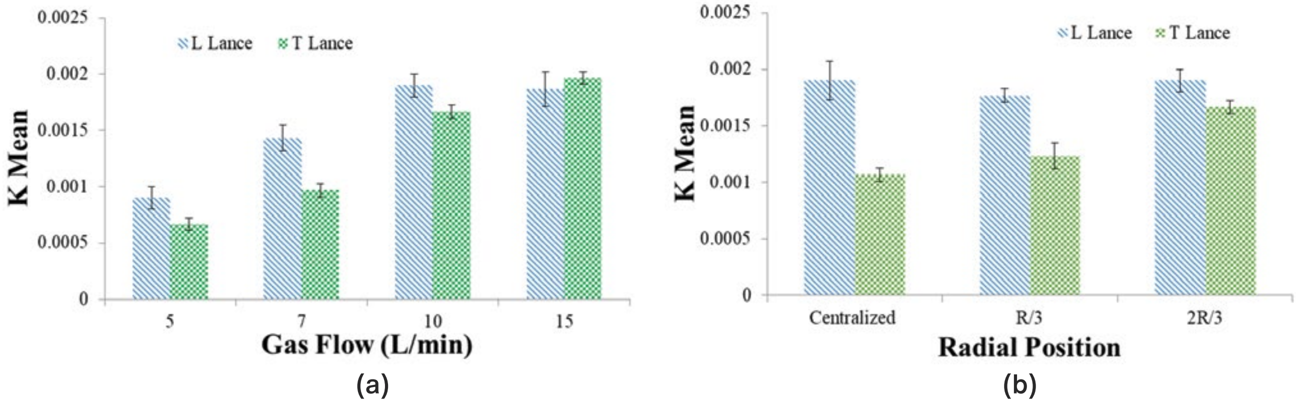

Figure 9

Comparison of the slag eye opening with the submerged lance shaped in L or T at 10 lpm.

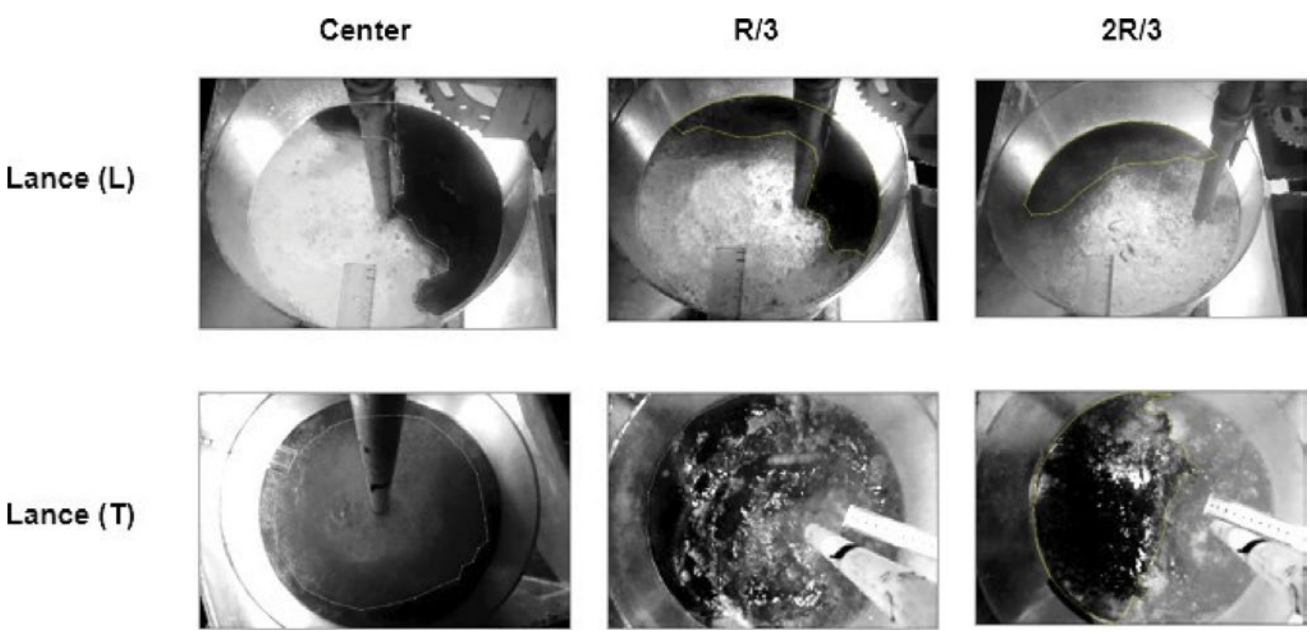

is directed perpendicularly to the ladle center. Further investigations are necessary to gain a deeper understanding of these correlations.

The curves representing the ratio of the slag eye opening area to the ladle surface area, considering the geometry in the analyzed image, are presented in Fig. 10, similar to the study conducted by Cruz et al.,[17] for each gas flowrate studied with the L- and T-shaped submerged lances at the three radial positions. An increase in the plume eye opening area was observed with increasing gas flowrate under all presented conditions. It was noted that the L-shaped lance has an orthogonal gas outlet, directing the flow from the 2R/3 position toward the center and from the central position toward the edge of the ladle, altering the fluid dynamic conditions of the lance's radial positions. The 2R/3 position for the T-shaped lance exhibited the smallest eye opening for the highest gas flowrates. Further studies on bubble size can contribute to deepening the understanding of the fluid dynamic phenomena. Additionally, it was observed that the plume eye size begins to enter a stability zone at higher flowrates. However, it is in this zone that the largest plume eye opening measurements were recorded, as also noted by Li et al.[7] The plume eye diameter is affected by the

Figure 10

Comparison between the slag eye opening and the gas flowrate.

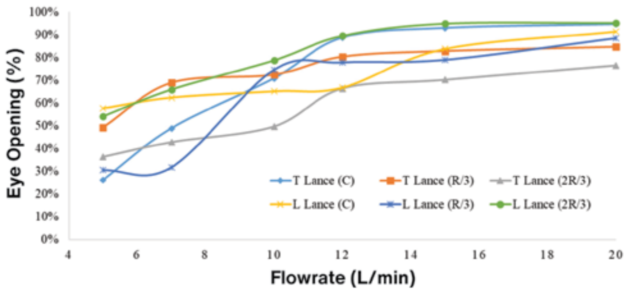

slag layer thickness near the meniscus region. However, it does not influence the axial velocity along the plume height for a given gas flowrate.[12]

Li et al.[7] studied the effects of gas flowrate through a porous plug on plume eye opening. The results show that the higher the inert gas flowrate, the more stable the plume eye becomes; however, increasing the gas flowrate also results in a larger plume eye opening. Other studies have addressed the same topic but focused on fixed lances, with findings indicating that lance morphology has a significant influence on bubble distribution, plume volume and eye opening. In the study of Cruz et al.,[17] a lance with a single vertical hole exhibited the smallest plume eye opening and the lowest plume volume, while a disk-shaped lance presented the largest plume eye opening and the highest plume volume.

Conclusions

Data from a physical model of the desulfurization ladle with gas injection through a submerged lance in L-shape (single hole) or T-shape (inverted T, two holes) were analyzed. It can be concluded that:

- Regarding the mixing time analysis, the results show that the most decentralized position resulted in shorter mixing times, while the centralized position exhibited the worst condition for both outlet configurations of the submerged lance. It was observed that under the same radial position and immersion depth conditions, the T-shaped submerged lance achieved shorter homogenization times.
- The mixing time decreases with higher energy input values, meaning that higher gas flowrates injected into the system result in shorter mixing times. Additionally, a larger influence of energy input on mixing time was observed at the R/3 radial position for both lance designs. Between the two submerged lance outlet designs, the T-shaped outlet exhibited a larger influence of energy input on mixing time.
- An increase in gas flowrate resulted in larger thymol extraction from water into oil. Moreover, the 2R/3 radial position yielded superior results compared to the other positions. Also, it was observed that the T-shaped design of the submerged lance exhibited lower thymol extraction under the same experimental conditions, concluding that the L-shaped lance was more efficient in the mass transfer process. The evaluation of the K_{ap} (apparent mass transfer coefficient) highlighted that this coefficient was higher across all flowrates for the L-shaped submerged lance. This effect can be justified by the higher gas exit velocity in the single-hole lance, which promotes oil dispersion into smaller droplets, consequently increasing the surface area for thymol absorption.
- A direct relationship between slag eye opening and gas flowrate was observed. Additionally, the most decentralized position of the L-shaped submerged lance exhibited a larger slag eye opening, whereas for the T-shaped submerged lance, the most decentralized position resulted in a smaller slag eye opening. Finally, it is concluded that the slag eye size begins to enter a stability zone at higher gas flowrates, and it is in this zone that the largest slag eye opening measurements are recorded.

This article is available online at AIST.org for 30 days following publication.

References

1. M.A. Silva, "Evaluation of the Use of Calcium Carbide-Based Desulfurizing Agents Containing Sodalite as a Substitute for Fluorite in Torpedo Ladles," (in Portuguese) master's thesis, Universidade Federal de Minas Gerais, 2012.
2. A. Ghosh and A. Chatterjee, *Ironmaking and Steelmaking, Theory and Practice,* PHI Learning Private Ltd., New Delhi, India, 110001, 2008.
3. P.A. Sá, "Slag-Metal Behavior in a Steel Refining Ladle Agitated by Inert Gas Bubbling," (in Portuguese) master's thesis, Federal University of Ouro Preto, the Center for Technological Education and the State University of Minas Gerais, 2015.
4. Z.C. Xin, J.S. Zhang, K.X. Peng, J.G. Zhang, C.H. Zhang and Q. Liu, "Modelling of LF Refining Process: A Review," *Journal of Iron and Steel Research International,* 2023, pp. 1–29.
5. A. Ghosh, *Secondary Steelmaking, Principles and Applications,* CRC Press LLC, 2001.
6. Q. Cao, L. Nastac, A. Pitts-Baggett, Q. Yu, "Numerical Investigation of Desulfurization Kinetics in Gas-Stirred Ladles by a Quick Modeling Analysis Approach," *Metallurgical and Materials Transactions B*, 2018.

7. L. Li, "Water Model and CFD-PBM Coupled Model of Gas-Liquid-Slag Three-Phase Flow in Ladle Metallurgy," *ISIJ International,* Vol. 55, No. 7, pp. 1337–1346. 2015.
8. X. Wang, S. Zheng and M. Zhu, "Optimization of the Structure and Injection Position of Top Submerged Lance in Hot Metal Ladle," *ISIJ International,* Vol. 61, No. 3, 2021, pp. 792–801.
9. S. Torres, "Numerical Simulation of an Argon Stirred Ladle With Top and Bottom Injection," *Open Journal of Applied Sciences,* Vol. 6, 2016, pp.860-867.
10. D. Mazumdar and R.I.L. Guthrie, "Mixing Models for Gas Stirred Metallurgical Reactors," *Metallurgical Transactions B,* Vol. 17B, 1986.
11. X. Zhou, Y. Zhang, Q. He, P. Ni, Q. Yue and M. Ersson, "Novel Evaluation Method to Determine the Mixing Time in a Ladle Refining Process," *Metallurgical and Materials Transactions B,* Vol. 53, 2022, pp. 4114–4123.
12. F. Tan, Z. He, S. Jin, L. Pan, Y. Li and B. Li, "Physical Modeling Evaluation on Refining Effects of Ladle With Different Purging Plug Designs," *Steel Research,* 2020.
13. Q.N. Hoang, M.A. Ramirez-Argaez, A.N. Conejo, B. Blanpain and A. Dutta, "Numerical Modeling of Liquid-Liquid Mass Transfer and the Influence of Mixing in Gas–Stirred Ladles," *JOM,* 2018.
14. Q. Cao and L. Nastac, "An Innovative Modeling Approach for Predicting the Desulfurization Kinetics in Na Argon-Stirred Ladle Furnace," The Minerals, Metals & Materials Society, 2018.
15. A.N. Conejo, *Physical and Mathematical Modelling of Mass Transfer in Ladles due to Bottom, Gas Stirring: A Review,* University of Science and Technology, China, June, 2020.
16. D. Mazumdar, *A First Course in Iron and Steelmaking,* 1st ed., Universities Press, Telangana, India, 2015, p. 380.
17. S.D. Cruz, M.A. Barrom, D.Y. Medina and J. Reyes, "Lance Design for Argon Bubbling in Molten Steel," *World Journal of Engineering and Technology,* Vol. 8, 2020, pp. 317–328.
18. J. Szekely and N. El-Kaddah, "Mathematical Model for Desulphurization Kinetics in Argon-Stirred Ladles," *Ironmaking and Steelmaking,* Vol. 8, No. 6, 1981, pp. 269–278.
19. D.B. Perasoli, C.L. Silva, C.B. Filho, M.C.S. Silva, J.J.M. Peixoto and C.A. Silva, "Physical Modeling of Hot Metal Desulfurization Through Submerged Rotative Lance," *AISTech 2023 Conference Proceedings,* 2023, pp. 876–883.
20. A.M.B. Silva, M.A. Oliveira, J.J.M. Peixoto and C.A. Silva, "Slag-Steel Emulsification on a Modified RH Degasser," *Metallurgical and Materials Transactions B: Process Metallurgy and Materials Processing Science,* Vol. 52, No. 4, 2021, pp. 2111–2126.

AISTech This paper was presented at AISTech 2025 — The Iron & Steel Technology Conference and Exposition, Nashville, Tenn., USA, and published in the AISTech 2025 Conference Proceedings.